Registry No. PE, 9002-88-4; PS, 9003-53-6; PO, 25068-38-6; PP, 9003-07-0; PBA, 9003-49-0; PVME, 9003-09-2.

References and Notes

(1) See the previous paper in this journal.
(2) Flory, P. J.; Orwoll, R. A.; Vrij, A. *J. Am. Chem. Soc.* **1964**, *86*, 3507.
(3) Somcynsky, T.; Simha, R. *Macromolecules* **1969**, *2*, 343.
(4) Nanda, V. S.; Simha, R. *J. Phys.* Chem. **1964**, *68*, 3158. Prigogine, I.; Traffeniers, H.; Mathot, V. *J. Chem. Phys.* **1957**, *26*, 751.
(5) Jain, R. K.; Simha, R.; Zoller, P. *J. Polym. Sci., Polym. Phys. Ed.* **1982**, *20*, 1399.
(6) Zoller, P. *J. Polym. Sci., Polym. Phys. Ed.* **1982**, *20*, 1453.

Dynamics of Rodlike Macromolecules in Nondilute Solutions: Poly(*n*-alkyl isocyanates)

G. T. Keep† and R. Pecora*

Department of Chemistry, Stanford University, Stanford, California 94305.

Received June 23, 1987; Revised Manuscript Received September 14, 1987

ABSTRACT: Theories of caging of rigid rodlike molecules of length L and diameter d in semidilute solution are extended to higher concentrations. Packing considerations indicate that ordering in concentrated rigid rod systems must occur below $CL^2d = 2.26$, where C is the number concentration of rods. In addition, the concentration at which the mean square deflection of a semiflexible polymer chain is equal to the cage size is calculated in terms of the ratio of the persistence length to the contour length. These and other considerations are used to interpret a series of dynamic light scattering experiments on solutions of low molecular weight samples of poly(*n*-butyl isocyanate), poly(*n*-hexyl isocyanate), and poly(*n*-octyl isocyanate). Samples of these materials were fractionated by a recrystallization procedure that was developed to minimize complications due to the presence of water. The polymer fractions selected for study were characterized by capillary viscometry, differential refractometry, infrared and ultraviolet spectroscopy, vapor pressure measurements, and total intensity light scattering. The dynamic light scattering experiments in the semidilute region, as analyzed by the programs DISCRETE and CONTIN, usually give multimodal time correlation functions that are qualitatively interpreted in terms of caging theories and rotational–translational coupling. This coupling grows in importance in a fashion consistent with caging theories as the concentration is raised or the molecular diameter is increased. In the high CL^2d region the solutions studied form either a mesophase or a gel depending on the method of solution preparation and the molecular mobility (which depends in turn on other parameters such as the axial ratio and the flexibility).

I. Introduction

Since the seminal work of Doi and Edwards,[1-3] much work has focused on the dynamics of rigid rod and wormlike macromolecules in nondilute solutions. From a theoretical point of view, these systems provide ideal model systems for studying the interactions of polymers in solution since at a given volume fraction the rodlike shape maximizes the short-range intermolecular interactions that hinder rotational motions. Since at high volume fractions such systems often form liquid crystal phases, the factors that determine when and why such transitions occur and the behavior of the system immediately before the transition may be probed. Studies of concentration effects in such systems also provide insight into the interpretation of dynamic data from systems which cannot be studied at low concentrations such as micelles.[4] From a practical point of view, stiff rodlike macromolecules are the basis of new ultrastrong polymer materials.

Most current analyses of the dynamics of rodlike macromolecules in semidilute solution are based on the theories of Doi and Edwards[1-3] (referred to hereafter as DE). Doi and Edwards modeled the hard core interactions between perfectly rigid, thin rods in terms of the cages a collection of neighbors form around any particular rod. The cage prevents the enclosed rod from executing lateral translational motion or rotational motion outside of the cage boundaries until the rod escapes the cage or the cage dissolves by having rods diffuse along their length. This theory predicts that the rod rotational diffusion becomes highly hindered at relatively low rod concentrations and that, concurrently, the solution becomes highly viscous. This initial theory predicted a much more severe slowing down of the rotational diffusion and a much lower concentration for the onset of the slowing down than was actually observed in systems that more or less approximated rigid rod systems, but it did give a qualitatively correct description of the phenomenon.

Subsequent work has utilized the original caging assumption of the DE theory but has refined some of the details. These efforts may be classified on the basis of what aspect of the original theory they modify. These are (1) cage escape mechanisms,[5] (2) effects of the molecular flexibility that exist in even rather rigid systems,[6] and (3) recalculation of cage sizes and geometry.[7-9]

In a previous paper we showed that a more detailed description of the cage geometry expected for infinitely thin rigid rods gave a substantial improvement in the agreement between experiment and theory but was not sufficient to resolve all the major discrepancies.[9] It appears that in order to bring theory into agreement with experiment within the framework of caging theories, it is necessary to introduce refinements (1) and (2) mentioned above, although this is very difficult to do quantitatively. In section II of this paper, our earlier work on cage characterization[9] is extended to show when flexibility and finite diameter should have significant effects on rod dynamics.

In section III the characterization and the preparation of solutions for light scattering of a series of short, thin and rigid poly(*n*-alkyl isocyanates) of varying diameter are described as well as the light scattering apparatus and data

† Present address: Tennessee Eastman Company, P.O. Box 1972, Kingsport, Tennessee 37662.

0024-9297/88/2221-0817$01.50/0

analysis techniques. In section IV, the results of total intensity and dynamic light scattering experiments on the polymer solutions are given. In section V, the results are discussed in terms of current theories of the dynamics of rodlike polymers in semidilute solution, including the extensions to them discussed in the first part of this paper.

II. Extensions of Caging Theory

In a previous paper,[9] we presented a model for calculating the size of cages formed in solutions of infinitely thin rods as a function of CL^3. These cages, formed by the other rods in solution, confine a test rod and limit its rotational motion until translational motion along the rod axis dissolves the cage and forms a new one.

In this model the only interaction between the infinitely thin rods is that they cannot pass through each other. The test rod motion was simplified by modeling its rotation by observing the motion of its tip on an enveloping sphere. The blocking segments of neighboring rods can then be geometrically mapped onto the surface of this sphere in a straightforward way. This procedure was used to calculate the average solid angle through which the test molecule can rotate (the cage size) at a given CL^3:

$$\langle \Omega \rangle = \frac{256}{\pi\left\{(CL^3)^2 - \left(\frac{836}{15\pi}\right)(CL^3)\right\}} \qquad (1)$$

The important observation was made that according to this model rods are not generally caged below normalized number concentrations $CL^3 = 17$; they are generally caged around $CL^3 = 35$ and almost always caged above $CL^3 = 50$. The rotational diffusion coefficient for infinitely thin rods was also calculated by using the cage escape mechanisms originally proposed by DE. Although more sophisticated cage escape mechanisms that have been presented in the literature may be used to further refine this calculation, we here are concerned mainly with using the geometric result given in eq 1 to consider the effects of finite diameter on orientational ordering and when corrections for molecular flexibility become significant. These considerations are used in the interpretation of the light scattering experiments on the poly(*n*-alkyl isocyanates) in section V.

Finite Diameter Effects. Randomly oriented rods do not efficiently pack. Forcing them into small volumes eventually acts to orient them producing a more efficiently packed structure—the liquid crystalline phase. In the caging considerations presented previously,[9] the rods were considered to be infinitely thin and hence not subject to the forces that produce liquid crystal phases. Thus, in the model the rods were considered to have completely random orientations. It is however a relatively simple matter to determine the concentration at which a collection of rods occupying a given volume must begin to exhibit some orientational order.

Edwards and Evans[10] have treated the dynamics of rodlike randomly oriented systems at high concentrations. At such concentrations, finite diameter effects should become important, especially the effect of end-on collisions which could lead to "log-jamming". These calculations, as they emphasize, include the admittedly nonphysical assumption that rods at such high number concentrations remain randomly oriented. We find here the concentration at which this is no longer possible and non random packing must occur.

Equation 1 gives the average solid angle of a cage as a function of concentration and rod length. Consider such a cage (assumed to be a square for convenience) with a single rod at its center. Now imagine the diameter of the test rod, as well as the blocking rods, growing in diameter until they touch exactly framing the test rod. The side of the square will be exactly twice the largest possible diameter. We then find the solid angle of such a square on the surface of a sphere of radius $(L/2)$, set it equal to the solid angle given by eq 1, and solve for the maximum concentration at which a rod barely fits in the typical cage. Thus

$$\langle \Omega \rangle = \frac{(2d)^2}{(L/2)^2} = \frac{256}{\pi\left\{(CL^3)^2 - \left(\frac{836}{15\pi}\right)(CL^3)\right\}}$$

which gives

$$CL^3 = \frac{418}{15\pi} + \left[\left(\frac{418}{15\pi}\right)^2 + \left(\frac{16}{\pi}\right)\left(\frac{L}{d}\right)^2\right]^{1/2} \qquad (2)$$

The maximum concentration for random packing vs the axial ratio as given by eq 2 is plotted in Figure 1. Note that the result is meaningless in the limit of small L/d since the calculations assume long rods.

For large L/d, the plot of CL^3 vs L/d in Figure 2 approaches a straight line with slope 2.26. Thus, for a collection of rods with random positions and orientations, one must always have

$$CL^2d < 2.26 \qquad (3)$$

Equation 3 of course gives an absolute limit. Ordering could (and probably does) occur before this concentration is reached. We conclude that it is impossible to have a randomly oriented and positioned collection of rigid rods at concentrations $C \gg 1/dL^2$. This does not mean that a liquid crystal transition must necessarily take place above this concentration. It is possible, for instance, that the system could develop significant orientational correlations between nearby molecules before becoming a liquid crystal. The theories of Onsager[11] and Flory[12] predict that liquid crystal ordering should occur at $CL^2d > 4$–6 which is two

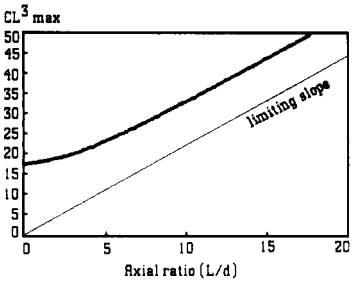

Figure 1. Plot of maximum concentration for random packing of cylinders as a function of axial ratio, based on cage sizes. This curve approaches a straight line with slope given by the thinner line.

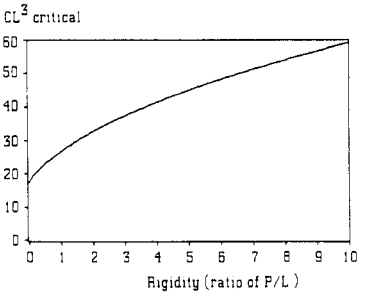

Figure 2. Plot of concentration at which cage size equals the mean-square fluctuation given by the wormlike coil model, as a function of the rod rigidity which is defined here as the ratio of persistence length to rod length.

to three times higher than the concentration derived above. Our result shows that solution ordering is probably important at much lower concentrations and should, therefore be considered in the dynamic theories.

Flexibility Effects. The flexibility of a rodlike molecule could have important effects on its rotational motion. In fact, the deviations observed between theory and experiments on semidilute solutions are often ascribed to flexibility.[13] Although most of the molecules studied are relatively stiff, they may exhibit enough flexibility to invalidate the assumption that they are able to be caged by a relatively few blocking points. For instance, a flexible end of a rodlike molecule is, to some extent, free to choose its own path when translating along its length despite the fact that the trailing portions of the molecule may be caged and hence restricted to a certain orientation.

The wormlike coil theory of Kratky and Porod[14-18] has been used to model the structure and dynamics of semistiff rods in dilute solution. Doi[8] has applied this model to calculate the dynamics of a rod as a function of flexibility in the limiting case of very high concentration. This theory does not address the question of the concentration dependence.

The Kratky–Porod model treats the polymer chain as a continuous elastic wire characterized by a "persistence length". If a unit tangent vector to the chain is placed at position 0 along the chain contour and another at position s, the expectation value of the dot product of these two unit vectors is given by

$$\langle \hat{\mathbf{u}}(0)\cdot\hat{\mathbf{u}}(s)\rangle = \exp(-s/P) \tag{4}$$

where P is the persistence length.

It is shown in the above references that the mean-square deflection from linearity of such a piece of the wormlike chain is given by

$$\langle \xi^2(s)\rangle = \frac{2s^3}{3P} \tag{5}$$

for small s/P.

Odijk has modeled the dynamics of a wormlike coil in a solution of intermediate concentration.[6] He first treats a wormlike coil trapped in a porous medium and then extends this theory to the case of the coil in a medium composed of the enmeshed neighboring coils. Odijk argues that when the mean-square deflection of a coil is smaller than the solution cage size, the molecules behave as predicted in the rod models. However, when the coil is able to bend outside the supposed confines of the cage, the hindering effect on the molecular rotation will be much less than that predicted for completely rigid rods.

Odijk uses the original DE formulas for calculating cage sizes. He, however, calculates the cage size around a coil segment one persistence length long, since such segments are presumed to rotate independently. The concentration dependence of the rotational diffusion coefficient, θ, cancels out in this regime, giving

$$\theta \sim kT/\eta PL^2$$

Note the much weaker dependence of θ on length than that predicted by the DE theory for rods.

We here use eq 1 to find the concentration at which the cage size is the same as the mean-square deflection of the wormlike coil. This signals the transition to a new dynamical regime. The direct applicability of Odijk's results is discussed further in section V.

If the center of a rod has a fixed orientation, then the radial segment of the rod which contributes to the deflection has length $L/2$. Hence the solid angle can be found and substituted into eq 1 as before to give

$$\langle\Omega\rangle = \{2(L/2)^3/3P\}/(L/2)^2 = \frac{256}{\pi\left\{(CL^3)^2 - \left(\frac{836}{15\pi}\right)(CL^3)\right\}}$$

which, when solved for CL^3 as a function of P/L, gives

$$CL^3 = \left(\frac{418}{15\pi}\right) + \left[\left(\frac{418}{15\pi}\right)^2 + \left(\frac{768}{\pi}\right)\left(\frac{P}{L}\right)\right]^{1/2} \tag{6}$$

Equation 6 is plotted in Figure 2. Note that in the limit of P/L approaching zero, the equation is meaningless since in this limit the molecules are random coils and the caging conditions are no longer valid. The region near $P/L = 1$ is particularly interesting since this is a typical degree of flexibility of the polymers studied by several research groups. At $P/L = 1$, the critical concentration is only $CL^3 = 26.85$. Even for the rather stiff case of $P/L = 10$, the critical concentration is only $CL^3 = 59.1$.

Given these results and the persistence lengths of common polymers, it is unlikely that the dynamics of solutions of rodlike polymers at concentrations above $CL^3 = 60$ could be understood without taking into account the flexibility of the molecules. The molecular flexibility is an important factor in determining the caging efficiency in systems that are usually studied.

Dynamic Considerations. Two points of view have emerged over the question of how the dynamics of rod motion in a caging environment should be treated. One is that the basic picture of Doi and Edwards is correct, but further refinements on the complex details of cage escape mechanisms are necessary. The other is that the caging concept is irrelevant to the dynamic process and that mechanisms other than cage escape dominate the orientational relaxation.

Teraoka et al.[5] have focused on more sophisticated treatments of cage escape mechanisms. They describe the rotational motion as a series of discrete hops between cages when gates open between them. This mechanism results in complicated expressions for the rotational relaxation time which, however, reduce to simple scaling laws upon numerical calculation. Fixman[19] has espoused the other point of view, which is based on the observation that the dissipation of forces in an entangled rod system may be much faster than diffusive motion. Furthermore, binary collisions alone may be sufficient to describe the relaxation of molecular orientation. Fixman's considerations lead to an expression for the rotational friction coefficient, ζ, at concentration C minus that at low concentrations, ζ_0.

$$\zeta - \zeta_0 \propto CL^3 \tag{7}$$

The DE theory predicts that ζ varies as the square of CL^3. Fixman supports his analytical results with computer simulations that pay careful attention to the step size used. There are, however, significant differences between the results of Fixman's simulations and those of Frenkel and Maguire[20] and Magda, Davis, and Tirrell.[21] These latter groups of authors simulated a pure fluid of infinitely thin rods rather than rods immersed in a viscous continuum. The pure fluid simulation results (with some modifications to estimates of the cage escape times appropriate to a pure fluid) are consistent with the Keep–Pecora modification of the Doi–Edwards theory. In particular, Magda et al.[21] find that the transition to semidilute behavior occurs at $CL^3 > 70$, although molecular interactions significantly affect the diffusive motion of the rods. Although the experimental work of Mori et al.[22] is consistent with the prediction of eq 7, most of the existing experimental work

Table I
Viscometry Results

system	[c], dL/g	Huggins k'	L,[a] Å	MW, g/mol
POIC in cyclohexane	1.45 ± 0.01	0.46 ± 0.02	774 ± 2	60 000 ± 140
big PHIC in cyclohexane	6.3 ± 0.2	0.68 ± 0.06	1610 ± 20	102 000 ± 1000
small PHIC in cyclohexane	1.92 ± 0.03	0.42 ± 0.05	830 ± 4	52 700 ± 300
PBIC in chloroform	1.9 ± 0.2	0.42 ± 0.08	750 ± 30	37 000 ± 1300

[a] L Based in Kirkwood formulas with diameters taken to be 18, 14, and 10 Å. Molecular weight is based on L with L/monomer taken to be 2 Å.

Table II
Results from Vapor Phase Measurements

quantity	POIC	big PHIC	small PHIC	PBIC
solvent	cyclohexane	cyclohexane	cyclohexane	chloroform
MW (g/mol)	11 900 ± 700	14 600 ± 700	6700 ± 110	6800 ± 2500
L (Å) from MW[a]	154 ± 9	230 ± 11	106 ± 2	140 ± 50

[a] L derived from the molecular weight assumes a rod with 2 Å/monomer.

gives results that are at least in qualitative agreement with modifications of caging theories.

III. Experimental Section

Preparation and Characterization of the Materials. A series of poly(*n*-alkyl isocyanates) with the *n*-alkyl = *n*-butyl, *n*-hexyl, and *n*-octyl was chosen for this study because these molecules have high rigidities and small diameters. The persistence lengths, which vary with solvent polarity, range from 550 to 1600 Å,[23-26] while the diameters range from 10 Å for the *n*-butyl isocyanate[23] to an estimated 14 Å for *n*-hexyl and 18 Å for *n*-octyl. The alkyl groups are attached to nitrogen atoms which alternate down the chain backbone with carbonyl groups. These form a rigid helix[23-25] whose length per monomer is taken here to be 2 Å, a typical value reported in the literature. Bur and Fetters[23] have given a detailed critical review of the literature on these polymers up to the mid 1970s.

The samples used in this work were synthesized and donated by Dr. S. M. Aharoni of Allied Corp. using methods already described.[27] Only a relatively brief description of the fractionation and characterization of these samples is given here. Further details may be found elsewhere.[28]

The polymers were fractionated by a fractional crystallization procedure[29-31] that was modified to minimize the necessity of limiting their exposure to the atmosphere. In the usual methods, trace amounts of water absorbed from the atmosphere can cause phase separation of the solvent and nonsolvent that makes it difficult to observe and harvest precipitated polymer. The modified method, in fact, deliberately introduces water into the system. The samples were first washed by precipitation from a toluene solution with methanol in 60% yield. Then the samples were redissolved in tetrahydrofuran and precipitated stepwise via addition of water. The limit of molecular weight resolution obtainable by this procedure was probably not attained due to the necessity of obtaining relatively large amounts of sample for the rather extensive series of concentration dependence experiments reported below, although six to ten fractions of monotonically decreasing molecular weight were obtained for each polymer. Infrared spectra confirmed that the chemical compositions of the polymer chains were not modified by this procedure.

Four fractions were chosen for detailed study, one fraction of the *n*-octyl, one of the *n*-butyl, and two of the *n*-hexyl. They are here designated, respectively, as POIC, PBIC, big PHIC, and small PHIC. The POIC, small PHIC, and PBIC have approximately the same contour length but have varying diameters and stiffness.

Molecular Weights. Molecular weights were measured by a variety of techniques. Viscosities were measured as a function of concentration at 20 °C by using an Ubbelohde viscometer. The intrinsic viscosities and Huggins constants derived from these measurements are shown in Table I. The molecular weights and lengths were determined by using the Kirkwood equation[32] for the intrinsic viscosity of rigid rods

$$[\eta] = (4\pi N_A L^3)/(9 \times 10^3 M \ln (2L/d)) \quad (8)$$

where N_A is Avogadro's number and M is the molecular weight. The length in eq 8 was converted to a molecular weight assuming that, as discussed above, the length per monomer is 2 Å and the diameters for calculating the L/d ratio for the three different polymers are also as given above. Note for rigid rods, capillary viscometry gives an approximately *z*-average molecular weight (third moment) rather than the 1.5 to 2nd moment for flexible coil molecules.[33,34] The molecular weights presented in Table I agree with those derived from dynamic light scattering photon correlation measurements on dilute solutions of the samples within 3–25%. DLS photon correlation spectroscopy in combination with the Broersma relations[35] relating the measured translational diffusion coefficient to the rod length also yields an approximately *z*-average molecular weight.

Total intensity light scattering was also measured as a function of scattering angle by using an apparatus described elsewhere[36] with ambiguous results. The molecules were generally too small to obtain reliable radii of gyration. The small size coupled with the weak refractive index increments (dn/dC's) gave very weak scattering signals from the polymer (roughly equal to the pure solvent scattering) at the low concentrations required to correct for solution virial effects. Trace quantities of water absorbed from the atmosphere during the filtration process used to remove dust was observed to change the values of dn/dC by as much as 50%. Using the values of dn/dC obtained from solutions that were not exposed to the atmosphere and light scattering intensities measured on solutions that had been exposed to the atmosphere during filtration gave the unphysical result that the weight average molecular weights are about twice as big as those measured by viscometry and dynamic light scattering. Attempts to correct for the effects of small amounts of water by estimating values of dn/dC after a typical filtration procedure gave results consistent with the *z*-average results, but with very low precision.

Other effects on solutions of these polymers due to the presence of varying amounts of water are given in detail elsewhere.[28] These include effects on solution density and the phase separation of water upon rapid cooling from water-saturated solutions.[37] In the experiments described below measures were taken to minimize trace water contamination or, when unavoidable, to circumvent its effects.

Number average molecular weights were measured by using a Hitachi Perkin-Elmer Model 115 vapor phase molecular weight apparatus. The results are given in Table II. Since the molecular weights of these polymers are relatively high for application of this technique, a low instrumental response per unit mass and a relatively low precision in the results was obtained. Careful adjustment of the current through the thermistors in the measuring apparatus to avoid concentration gradients was done, as suggested by Bersted.[38] The number average molecular weights found by this method are about one-fourth the *z*-average values found from viscometry on carefully dried solutions. This discrepancy is probably due to a low molecular weight contaminant and not to trace water contamination, since the samples discussed were all carefully dried and other samples to which water was deliberately added gave very different results.

Ambler et al.[33] reported an acid-catalyzed depolymerization of isocyanate chains triggered by UV decomposition of a chlo-

Table III
Molecular Parameters Helpful in Interpreting Dynamic Light Scattering Results[a]

quantity	POIC	big PHIC	small PHIC	PBIC
solvent	cyclohexane	cyclohexane	cyclohexane	chloroform
solvent refractive index (20 °C)	1.426 62	1.426 62	1.426 62	1.4459
solvent viscosity (P) (20 °C)	0.0098	0.0098	0.0098	0.0058
M_0 (g/mol)	155	127	127	99
L_0 (Å)	2	2	2	2
d (Å)	18	14	14	10
MW (g/mol)	60 000 ± 140	102 000 ± 1000	52 700 ± 300	37 000 ± 1300
L (Å)	774 ± 2	1610 ± 20	830 ± 4	750 ± 30
L/d	43	115	59	75
Pd maximum	2.2	2.6	2.8	2.3
CL_z^3 (mg/mL)	4.67	24.5	6.53	6.81
R_h (Å) calcd	103	170	102	87

[a] d and d/monomer (L_0) are estimates; MW and L are based on viscosity data and are therefore z averages (for rods). Maximum polydispersity (Pd) is taken to be the square root of the ratio of MW from viscometry to MW from vapor phase measurements. R_h is the calculated value based on the given parameters.

roform solvent. We observed that contact of the polymer solutions with platinum (which was used in the original fittings in the vapor phase molecular weight apparatus) caused no immediate change in the DLS or UV spectra but that 1 month after the platinum was removed, the UV spectra changed markedly, which could be explained by a slow depolymerization after an initial attack by the platinum. The high 40% of the material that was methanol soluble and was removed in the wash step before fractionation also supports the possibility of the presence of low molecular weight material in the final samples.

If one chain in 50 depolymerized after fractionation, this could make the molecular weight results consistent. It is likely that the samples were composed of a relatively narrow collection of undamaged chains (polydispersity, as defined by the ratio of the weight average molecular weight to the number average, about 1.2) and less than about 1% of the material in various stages of depolymerization. The monomers and oligomers present would be essentially invisible in the light scattering and viscometry experiments.

In interpreting the DLS experiments reported below, experimental parameters based on the z-average molecular weights derived from the viscometry measurements (which we consider to be the best estimates) are used. These are shown in Table III. As may be seen from the table, three of the samples consist of chains about 800 Å long (about one-half persistence length in nonpolar solvents) and one about twice this length. Table III also lists the estimated maximum polydispersities of the samples (P_d maximum), the conversion factors CL_z^3/(mg/mL) used for converting concentration between CL^3 and mg/mL units and the hydrodynamic radii at 20 °C calculated from the Broersma relations,[35] the given size parameters, and the pure solvent viscosities. The maximum polydispersity of these samples, as is discussed above, is not well-determined. It would be difficult to take into account in the interpretation of the dynamic experiments even if it were more precisely known.[39]

Cyclohexane was chosen as the solvent for the DLS experiments because of its relatively high viscosity (to slow down the polymer dynamics), low index of refraction (to give more scattered intensity), and its relatively high polymer solubility. The POIC appeared to be the most soluble and the PBIC the least. In fact, the viscometry studies indicated that the PBIC tended to aggregate in cyclohexane, so that the DLS experiments for this polymer were performed, in addition, in chloroform. The persistence lengths should be at their highest in the nonpolar solvent cyclohexane, while the PBIC should be less rigid in the polar chloroform. The differences in solubility in the cyclohexane series seemed to correlate with the measured Huggins constants (Table I) (which in turn are probably related to the molecular rigidity) and also with the filtration times through 0.22-μm pore filters as described below.

Solutions were cleaned for light scattering by filtration through 0.22-μm Millipore filters and were checked for particulates ("dust") by observing a laser-illuminated volume of the sample under a low power microscope. Most solutions were free of particulates to a level of approximately one speck at a time in the 1-cm path of an unfocused 1-W argon ion laser beam. The solutions with the highest polymer concentrations and the highest viscosities had the highest dust levels. This may have been due to the gradual accumulation of airborne particles or to the formation of aggregates after filtration. Some solutions did show a concentration drop after filtration as monitored by UV–vis absorption spectra. During the filtration process, all samples were exposed to the atmosphere.

Table IV
Largest Observed Concentrations in CL^3 and CL^2d Dimensionless Units That Fit into Each of Several Classifications Based on Macroscopic Handling Characteristics[a]

polymer	solvent	forms gel	thick fluid	slow filter	easy filter
PBIC	THF	52/0.70			
PBIC	cyclohexane	18/0.24		7.5/0.10	4.1/0.054
PBIC	chloroform			75/1.0	51/0.68
small PHIC	cyclohexane	263/4.4	90/1.5	76/1.3	31/0.52
big PHIC	cyclohexane		127/1.1	83/0.72	47/0.41
big PHIC	cyclohexane satur.[b]			270/2.3	65/0.56
POIC	cyclohexane		315/7.3	89/2.1	59/1.4

[a] "Thick fluid" means flows under its own weight but cannot be forced through a 0.22 μm pore filter. Length is based on viscosity measurements. Diameters are taken to be 10, 14, and 18 Å for PBIC, PHIC, and POIC, respectively. [b] Water saturated cyclohexane.

In addition to its primary use in cleaning the solution of particulates, the filtration rates also provide qualitative information about solubility limits and polymer entanglements. In the case of dilute solutions and pure solvents, a pressure difference of much less than 0.5 atm across the filter sufficed to cause filtration to proceed at a rate in excess of 1 drop of solution per second. As the concentration of solution is increased by factors of 2, a concentration is reached in which more than 2 atm of pressure is suddenly required to cause the filtration to proceed at rates as slow as 1 drop per minute or slower. A further increase in concentration by a factor of 2 produced solutions that flowed under their own weight and were usually transparent but would not pass through the filters even under high pressure. A further increase in concentration by a factor of 2 would sometimes produce a transparent solution at high temperatures that would gel on cooling, turning opaque, and that would then no longer flow under its own weight. This latter behavior was reversible upon heating.

Table IV presents the concentrations at which these four distinct regimes were observed: gel, thick unfilterable fluid, slow filtering fluid, and the highest concentration of easiest filtering fluid. Values are given in terms of normalized concentrations CL^3 and CL^2d.

Note that a water-saturated solution of big PHIC in cyclohexane could be filtered at a much higher concentration than the normal solutions. The big PHIC and the POIC were not observed to gel at any concentration that could be made to dissolve at high temperature, possibly because they may have higher molecular

flexibility than the other samples.

Depolarized Total Intensity and DLS Measurements. Most of the DLS measurements were performed on an apparatus designed to optimize the measured signal with a fixed 90° scattering angle. The light source was a Spectra Physics Model 165 argon ion laser operating at 488.0 nm. The incident light beam was vertically polarized to better than 1%. The scattered light was always passed through a Glan-Thompson polarizer with extinction ratio about 10^{-5} before detection. The detection photomultiplier was an EMI 9893A/350 specially selected for low dark count and afterpulsing. The photomultiplier output passed through a SSR 1105 photon counter–discriminator system and then to a Brookhaven Instruments Model 2020 autocorrelator. Analysis of the autocorrelation functions was performed by a Universe 68 microcomputer manufactured by Charles River Data Systems. Depolarized total intensity measurements were done on the same samples as the DLS ones using this apparatus. All of these measurements were performed at a 90° scattering angle. A few measurements reported below were done on a variable scattering angle DLS apparatus described elsewhere.[40]

The effect of signal level was seen to dominate coherence effects,[28] such that the largest signal usable by the 4-bit memory registers in the autocorrelator without prescaling gave the best signal to noise ratio for a given run time. Typically, the irising aperture that defines the scattering angle was left at 1 mm opening, while the pinhole on the photomultiplier window that defines the scattering volume was varied to adjust the signal level from sample to sample. The argon ion laser was maintained in the light mode at 800 mW for maximum stability. The pinhole was varied between 50 and 1000 μm but was usually in the range from 200 to 500 μm, depending on the intensity of the scattered light and the time scales studied. The scattered light was never counted at more than four counts per sampling time and in the ideal case was set at one count per sample time. This prevented runs in which more than one count in a million or so overflowed the four bit register, ruining the correlation function.

Two different sampling schemes were normally used in the 80 channel Brookhaven correlator. The first used the first 72 channels, setting the sampling time to maximize the curvature in the early points of the correlation function. The base line was determined from the eight correlator delay channels. The second method used the "multiplexing" option of the correlator, whereby overlapping data sets are spliced together. The degree of multiplexing was chosen by collecting data on the fastest useful sampling time (0.5–1 μs) and using enough overlapping data sets to reach the base line. The first method gave the best signal to noise ratio, stability, and reproducibility while the latter gave the highest resolution of multiple decay mode correlation functions. Data was analyzed by the programs DISCRETE and CONTIN written by Provencher[41] and modified to run on our microcomputer by Bott.[42] DISCRETE fits the data to a sum of exponentials, and CONTIN fits it to a continuous distribution. In both cases algorithms in the program choose the number of exponentials (DISCRETE) or the number of peaks in the continuous distribution (CONTIN). Analysis by DISCRETE achieved the best resolution with the first sampling scheme, while CONTIN achieved the best resolution with the second method. CONTIN was, as expected,[41,42] often unable to resolve the number of modes present with the small number of data points produced by the first scheme.

It should be noted that the square root of the data minus the calculated base line was actually fit by these programs, since this is the quantity of most theoretical interest ($g^1(t)$). This procedure also accounts for any dust, heterodyning, etc. present. In all cases the first point of the correlation function was ignored.

Relaxation times are presented in terms of the hydrodynamic radius defined as

$$R_h = q^2kT/(6\pi\eta\Gamma)$$

where q is the scattering vector length, k Boltzmann's constant, T the absolute temperature, η the solvent viscosity at the temperature T, and Γ is the measured reciprocal relaxation time. The viscosity used here is always that of the pure solvent (0.98 cP at 20 °C and 0.90 cP at 40 °C for cyclohexane and 0.58 cP at 20 °C for chloroform). The index of refraction used in calculating the scattering vector length is 1.426 62 for cyclohexane and 1.4459 for chloroform (see Table III).

In all cases with sampling times less than 6 μs, a spurious relaxation time appeared in the measured relaxation time distribution at short times, usually one μs or less, but sometimes extending as far as 3 μs. This spurious time may arise from afterpulsing in the photomultiplier tube which becomes important for weakly scattering samples such as those studied here or perhaps from artifacts of the fitting programs. The contribution of these modes increased with faster sampling times and with the decreasing scattering power of the macromolecules at low concentration. This spurious fast relaxation time corresponds to hydrodynamic radii as high as 5–10 Å. The effect was visible even in correlation functions produced by direct scattering of light from glass surfaces without a solution present. Thus, any mode of motion with a hydrodynamic radius this small could not be distinguished from this artifact and so could not be reliably identified in our experiments if it were present.

In addition to this spurious mode at short times, at long times a mode due to dust sometimes appeared. Degrees of freedom were always allowed in CONTIN to account for this possibility. This was done by floating the base line parameter ("linear coefficient") and by setting the upper range of hydrodynamic radii (a range of radii in which CONTIN searches for the solution must be set) up to 3000–5000 Å. In general, the relative contributions of these dust modes were closely correlated with the amount of dust estimated from the microscope test described above.

The apparent hydrodynamic radii accessible in our experiments thus usually fall in the range between about 15 and 1000 Å.

IV. Results

Depolarized Total Intensity. Table V presents the total intensities measured at 90° scattering angle for all of the solutions studied. I_{VV} is the scattered intensity with both incoming and scattered light polarized vertical to the scattering plane (the "polarized component"). I_{VH} is that with the incoming light vertical and the scattered light horizontal (the "depolarized component"). The values given are the measured intensities minus the intensity in the corresponding component for the pure solvent at the same laser power normalized to the scattering from pure solvent. The depolarized component is more than an order of magnitude less than the polarized component. This may be seen from the depolarization ratio, ρ, defined here as the ratio of the unnormalized I_{VH} to I_{VV}.

The pure solvent depolarization ratios were measured and found to be 0.026 for cyclohexane and 0.12 for chloroform, in agreement with literature values.[43]

For ideal solutions I_{VV} and I_{VH} are proportional to the concentration, and ρ should be a constant. Deviations from this simple dependence are an indication of intermolecular correlations. Figure 3 is a plot of the depolarization ratio versus the number concentration times L^2d for the isocyanates. It is clear from this figure that the depolarization ratio is not a constant. In fact, for most of the solutions the depolarization ratio begins a systematic rise after a given concentration and that the point at which the rise begins for each solution varies with the molecular flexibility. At high concentrations, ρ appears to depend linearly on CL^2d. In this same region I_{VV}/C decreases from the dilute solution value, so that the main cause of the increase in the depolarization ratio appears to be the decrease in the polarized scattering per molecule. The depolarized scattering per molecule, however, rises slightly at even higher concentrations.

The molecular interpretation of this data is not yet clear. Since CL^3 is on the order of 50–100, many centers-of-mass lie within the reach of a given molecule. The decrease in the polarized intensity indicates intermolecular positional correlations among the rods (although the effects are such that a simple second virial series is inadequate to describe them), while orientational correlations do not appear to increase significantly until the higher concentrations.

Table V
Intensity Data, Polarized and Depolarized, Taken at 90° Scattering Angle[a]

C (g/mL)	I_{VV}	I_{VH}	ρ	I_{VV}/C	I_{VH}/C	ρ/C
			POIC			
19.4	1.98	2.73	0.0330	0.102	0.141	0.00170
12.7	2.05	2.11	0.0238	0.161	0.166	0.00187
8.3	1.59	1.06	0.0160	0.191	0.127	0.00193
7.5	1.72	0.89	0.0137	0.229	0.119	0.00183
4.5	1.28	0.50	0.0104	0.284	0.112	0.0023
2.79	0.94	0.27	0.0069	0.34	0.098	0.0025
1.8	0.56	0.19	0.0084	0.31	0.11	0.0047
			Big PHIC, Dry			
3.36	1.62	0.78	0.0124	0.48	0.23	0.0037
1.9	1.11	0.49	0.0113	0.58	0.26	0.0060
1.13	0.69	0.21	0.008	0.61	0.19	0.0071
0.54	0.28	0.13	0.012	0.52	0.24	0.022
0.297	0.11	0.09	0.02	0.4	0.3	0.07
			Big PHIC, Wet			
11	2.28	2.68	0.0309	0.207	0.244	0.00281
10	2.26	2.43	0.0283	0.226	0.243	0.00283
2.65	1.33	0.63	0.0125	0.502	0.238	0.0047
2.17	1.09	0.51	0.0124	0.502	0.24	0.0057
1.5	0.80	0.34	0.011	0.53	0.23	0.0074
0.66	0.40	0.21	0.013	0.60	0.32	0.021
0.29	0.17	0.05	0.007	0.60	0.17	0.03
			Small PHIC			
11.6	3.04	3.47	0.0319	0.262	0.299	0.00275
4.7	2.44	1.96	0.0175	0.519	0.417	0.00372
4.4	1.19	0.79	0.017	0.270	0.18	0.0039
3.4	0.79	0.61	0.019	0.23	0.18	0.0057
2.8	0.69	0.57	0.021	0.25	0.20	0.0074
0.88	0.23	0.09	0.010	0.26	0.10	0.011
0.64	0.17	0.07	0.010	0.27	0.11	0.016
			PBIC (Chloroform)			
11	1.14	0.32	0.034	0.104	0.029	0.0031
9.6	1.00	0.26	0.031	0.104	0.027	0.0032
5.9	0.70	0.15	0.029	0.12	0.026	0.0049
5.2	0.86	0.19	0.027	0.17	0.036	0.0052

[a] I_{VV}, I_{VH}, and ρ are defined in the text; T = 20 °C.

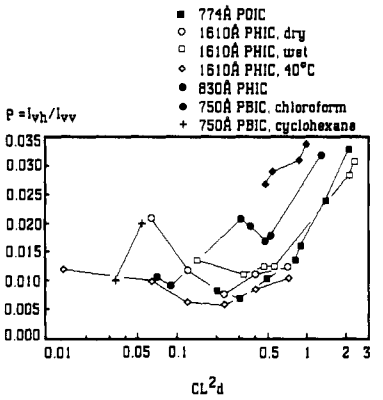

Figure 3. Plot of measured depolarization ratio (ρ) vs number concentration times length squared times diameter. The depolarization ratio is given by the ratio of the vertical–horizontal to vertical–vertical polarization scattering intensities, corrected for solvent scattering. Errors in ρ are largest at low concentration (>50%) and decrease to less than 1% for the higher concentrations. The plot clearly shows an increase in ρ at high concentrations for all solutions that correlate well with molecular flexibility and always occurs at less than the CL^2d = 2.26 predicted in section II.

Dynamic Light Scattering. The results for each of the samples are presented in Table VI, parts a through g and Figure 4, parts a through g.

The big PHIC (wet) sample in cyclohexane is of the same molecular weight as the big PHIC (dry). It was, however, prepared in a water-saturated state by exposing it to the steam in the atmosphere above a water bath for a few hours. Since higher concentrations could be filtered than for the corresponding "dry" sample, we suspect that the presence of water makes the PHIC somewhat more flexible. The DLS data are, however essentially the same for the two samples, but since higher concentration samples of the wet sample could be filtered, some data were obtained at rather high concentrations.

One or two modes were generally found for the polymer solutions studied. Three modes sometimes appeared as is discussed below.

The strongest mode typically corresponded to an R_h of 100–200 Å. For several of the samples the angular dependence (scattering vector length dependence) of the reciprocal relaxation time corresponding to this mode was studied. In all cases it showed a q^2 dependence and is hence probably due to translational diffusion of the macromolecule. The hydrodynamic radius also matches the radius predicted from the intrinsic viscosity to within 3–25%. This mode usually slowed down as concentration increased. We refer to it here as the "primary mode".

The second mode appeared only at high concentrations in conjunction with the slowing down of the primary mode. This mode relaxes somewhat faster than the primary mode and will be termed the "secondary mode". The relative intensity of the secondary mode grows steadily with increasing concentration. The precision in the measured reciprocal decay time of this mode was generally very poor compared to that for the primary mode, so that its angular dependence could not be established.

It should be noted that the ability to resolve these two modes plus the often present dust and fast modes depends not just on the signal to noise in the data but also on the

Table VI

concn			relaxatn modes: tertiary		secondary		primary	
(mg/mL)	CL^3	CL^2d	R_h, Å	amp., %	R_h, Å	amp., %	R_h, Å	amp., %
a. Polarized Dynamic Modes: POIC in Cyclohexane[a]								
19.4	91	2.11	25	16	72	78	280	6
12.7	59	1.38	34	20	93	80	←	
8.3	39	0.90	44	21	111	79	←	
7.5	35	0.81	12	3	78	70	263	27
4.5	21	0.49	12	2	80	66	197	32
2.79	13	0.30			52	30	145	70
1.8	8.4	0.20			42	17	123	83
b. Polarized Dynamic Modes: Big PHIC, Dry Solution[a]								
3.4	83	0.72	17	5	92	37	328	68
1.9	47	0.40			66	21	265	79
1.1	27	0.23			28	9	195	91
0.54	13	0.12			41	10	212	90
0.30	7.4	0.064			40	17	244	83
0.13	3.2	0.028			57	50	244	50
0.0604	1.5	0.013					187	100
c. Polarized Dynamic Modes: Big PHIC, Wet Solution[a]								
11	270	2.34	35	21	102	58	344	20
10	245	2.13	21	12	86	53	447	35
2.65	65	0.56	26	3	83	31	296	66
2.17	53	0.46	22	3	81	25	260	72
1.5	37	0.32			64	19	248	81
0.66	16	0.14			68	17	225	83
0.29	7.1	0.062					184	100
0.17	4.2	0.036					157	100
d. Polarized Dynamic Modes: Big PHIC, Dry, T = 40 °C[a]								
3.4	83	0.72			61	16	261	84
1.9	47	0.40			83	20	294	80
1.1	27	0.23			93	24	297	76
0.54	13	0.12			42	9	220	91
0.30	7.4	0.064			31	13	255	87
0.0604	1.5	0.013					167	100
e. Polarized Dynamic Modes: PBIC in Chloroform[a]								
11	75	1.00			47	68	165	32
9.6	65	0.87			56	65	157	35
5.9	40	0.54			55	54	200	46
5.2	35	0.47			62	59	214	41
2.8	19	0.25			53	36	144	64
1.36	9.3	0.12			20	16	115	84
0.748	5.1	0.068					91	100
0.51	3.5	0.046					101	100
0.170	1.2	0.015					104	100
f. Polarized Dynamic Modes: Small PHIC in Cyclohexane[a]								
11.6	76	1.28	534	7	29	26	54	67
4.7	31	0.52	560	11	29	13	62	75
4.4	29	0.48	272	1	←		57	99
3.4	22	0.37			20	7	96	93
2.8	18	0.31			15	2	85	98
0.88	5.7	0.097					90	100
0.64	4.2	0.070					87	100
0.35	2.3	0.039					76	100
g. Polarized Dynamic Modes: PBIC in Cyclohexane[a,b]								
0.6	4.1	0.054			67	71	196	29
0.375	2.6	0.034			77	70	202	30
0.201	1.4	0.018			←		124	100
0.085	0.58	0.0077			27	44	94	56
0.0216	0.15	0.0020					92	100

[a] Relaxation times are given in terms of apparent hydrodynamic radii. Amplitude is in percent of amplitude contribution to $g^1(t)$. [b] Note: poor solubility caused presence of macroscopic aggregates/dust. Strong slow modes were present, fit, and ignored, but this does affect the resolution of the data, and the accuracy of the concentrations quoted.

sampling scheme used. When care is not taken to chose the best time scales to ensure that adequate information for each mode is present in the raw data, the primary and secondary modes cannot be resolved. The resultant composite of the primary and secondary modes then often appears to relax faster with concentration after a possible initial slowing down. The behavior exhibited by this composite mode has been observed in other laboratories on similar systems to those studied here.[44,45] It is possible that they were also observing an unresolved composite mode. Since CONTIN is conservative in assigning modes that are not statistically justified by the information content of the correlation function and the fact that CONTIN does resolve the primary and secondary modes, it is unlikely (but not impossible) that they are artifacts of the data analysis program.

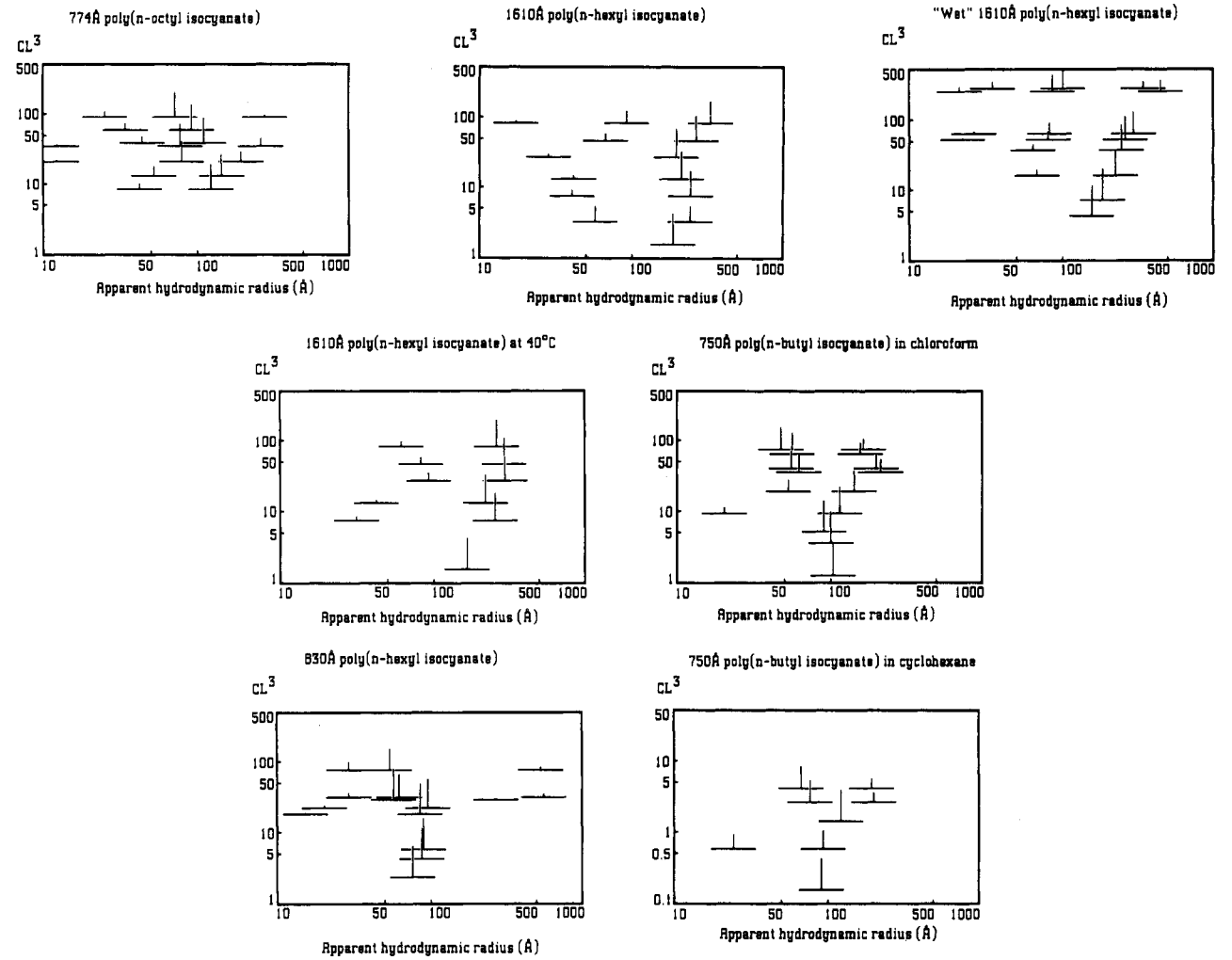

Figure 4. Polarized dynamic light scattering relaxation modes as a function of concentration: (a) 774 Å POIC; (b) 1610 Å PHIC, dry; (c) 1610 Å PHIC, wet; (d) 1610 Å PHIC, dry, $T = 40$ °C; (e) 750 Å PBIC in chloroform; (f) 830 Å PHIC; (g) 750 Å PBIC in cyclohexane. This sequence corresponds roughly to increasing rigidity. The base of the inverted T shows the concentration of the sample, the width corresponds to the factor of two size difference needed to resolve two narrow peaks, and the height is proportional to the percentage of the amplitude of $g^1(t)$ that relaxes with the indicated apparent hydrodynamic radius.

As mentioned above a third mode sometimes appears at high concentration in some of the solutions. In the small PHIC sample (Figure 4f), this is a very slow mode that appears in the 500–700 Å range. In the other solutions in which it appears (the big PHIC sample), it is a very fast mode that is somewhat slower than the fast artifacts. This mode is usually just on the border of statistically justifiable resolution.

In the presence of a slow third mode as was observed in the small PHIC sample, the primary and secondary modes are much more difficult to resolve. In fact, they are only resolved in the best data sets. DISCRETE is more likely to give this many modes than is the usually more conservative CONTIN, which often gives a broad smear of relaxation times when this many modes are present. CONTIN does show this many modes at low smoothing levels (0.1–0.3). Provencher[41] recommends setting the smoothing level at 0.5 while maintaining that solutions corresponding to values in the range 0.1–0.9 are significant possibilities. Bott, however, recommends lower smoothing levels (down to 0.2).[42] Thus, CONTIN indicates that these modes may be present, even quite likely, but in general will not assert with confidence that they are definitely present. Examples of raw data sets and DISCRETE and CONTIN outputs are given elsewhere.[28]

The depolarized time correlation functions generally exhibit much lower signal to noise ratios than the polarized ones. The positions of the modes, even when there is only one, are therefore much less precise than for the polarized spectra. Most of the samples show a mode that probably corresponds to molecular rotational diffusion. The POIC shows, in addition, a slow mode that could be attributed to dust or aggregates. It was not, however, seen in the polarized spectrum. The big PHIC (wet) shows a depolarized time correlation function much different from the corresponding dry sample. This sample had, in fact, the highest scattering intensities of any of those measured. Since the depolarized spectrum for this sample appears very similar to the polarized one, it is possible that polarizer leakage or multiple scattering is responsible for this depolarized spectrum.

The small PHIC exhibits the most unusual depolarized spectrum. The depolarized correlation function was dominated by very slow modes, which ranged in hydrodynamic radius from about 0.5 to 30 μm. If particles of such sizes were present they would have dominated the polarized spectra as well. The polarized spectra exhibited a slow mode but at much smaller hydrodynamic radii than those in the depolarized spectra (which, it must be emphasized, are very noisy and hence subject to artifacts). It is possible that there are regions of high orientational correlation present in these samples which could indicate that the system is near the composition for the separation of a liquid crystalline phase whose onset has not been detected

by more macroscopic techniques.[27,47]

V. Discussion

The primary mode in the polarized DLS correlation functions is almost certainly due to molecular translational diffusion. The DE theory includes the assumption that when molecules are caged, translational diffusion perpendicular to the long rod axis is prevented while there would be no effect on diffusion parallel to the axis. This assumption leads to the conclusion that, in the absence of solution virial effects, the translational diffusion coefficient in the semidilute regime should decrease to one-half its infinite dilution value. Zero and Pecora[46] found a decrease to two-thirds (although not monotonically) in solutions of poly(γ-benzyl-L-glutamate) (PBLG) in ethylene dichloride, while Russo[44] et al. observed an increase in D for solutions of PBLG in N,N-dimethylformamide (DMF). For samples with concentrations greater than $CL^3 = 100$, Russo et al. observed nonexponential correlation functions. Kubota and Chu[48] also studied PBLG in DMF and found increases in D followed by decreases at larger concentration. These latter authors also studied three molecular weights of PHIC in n-hexane.[49] Only one of their samples was in the low molecular weight range studied here. For this sample they found a slight linear increase in the translational diffusion coefficient in the semidilute region as measured by a cumulant fit to a polarized DLS time correlation function. Statman and Chu[31] also studied a sample of PBIC in carbon tetrachloride with a molecular weight about twice that of our PBIC sample. These authors found multimodal behavior throughout the concentration range studied. Jamieson et al.[45] found qualitative agreement with the Doi-Edwards predictions for semidilute solutions of xanthan polysaccharide ($L \sim 15000$ Å) in aqueous solution.

The results of Russo et al. are perhaps the most pertinent to those reported here.[44] These authors report a speeding up of the primary mode with concentration. They interpret this speeding up as an intermolecular solution virial coefficient effect, that is, that the solution is no longer thermodynamically ideal (ideality is assumed in the Doi-Edwards theory) and the mutual diffusion coefficient measured in DLS is no longer equal to the self diffusion coefficient. An analysis is presented that includes solution virial coefficient data obtained from integrated intensity light scattering to show that the self diffusion coefficient probably does slow down in the PBLG samples studied. In fact, it is concluded that it most likely slows down even more than predicted by Doi and Edwards. Their data appear in many respects like the data obtained here, except that our data analysis methods reveal multimodal time correlation functions. Single exponential fits to our data do indeed usually show a slight speeding up with concentration, except at the highest concentrations. In effect if we use oversmoothed solutions or if we force fit our data to single exponentials, we obtain relaxation times that behave qualitatively like those of Russo et al.

The common feature of our data and of much of the data in the literature is the appearance of multimodal DLS time correlation functions at high concentrations. As the concentrations increase the positions of the modes generally shift toward slower times while the relative intensity of the faster modes increase. In the case of the small PHIC, a very slow mode appears to arise independently of the others. When this mode appeared, it became more difficult to resolve the faster modes.

Several possible mechanisms for the appearance of multiple decay modes in DLS time correlation functions have been proposed in the literature. These include (1) contributions from rotational and internal modes of motion due to intramolecular form factor effects,[50] (2) polydispersity number fluctuations,[51] (3) anisotropic motion due to molecular crowding,[46,52] (4) formation of aggregates, and (5) a microphase separation, e.g., a microgel or a microdispersed liquid crystal phase.

It is unlikely that single molecule form factor effects could be the primary contributor to the observed DLS modes. Such effects should disappear at low values of the product of q and a characteristic dimension of the molecule. The largest molecule studied where such effects should be the most important is the big PHIC. Assuming that this molecule were a fully extended rod with the weight average molecular weight given in section III, we find that $qL = 4$ at a 90° scattering angle. A rod of this size would have a contribution of a mode including the rod rotational motion of about 3% of the total polarized scattered intensity. This intensity would be difficult to detect given the signal to noise ratios in these experiments. In addition, the actual contribution of the extra mode would probably be even less than this since the molecule is fairly flexible ($L/P = 1$–2.5) and the length estimate is based on the z-average molecular weight. Both of these factors should decrease the contribution of the rotational and internal modes to the time correlation function. These modes should also be present at low concentration.

Pusey and co-workers have proposed a mechanism for the appearance of an additional slow mode arising from a fluctuation in the distribution of molecular sizes present in the scattering volume of a polydisperse sample.[51] This effect has been observed in mixtures of polystyrene latex spheres.[53] This mechanism gives an additional contribution to the DLS time correlation function whose decay constant is determined by the translational self-diffusion coefficient. In the case of spherical molecules, this contribution usually decays more slowly than the contribution due to collective diffusion. Although the polydispersity mechanism observed in the latex sphere systems cannot be ruled out in the poly(n-alkyl isocyanate) solutions, there is no detailed theory applicable to mixtures of rodlike molecules whose results can be compared with those obtained here. It should be noted that bimodal DLS time correlation functions have also been observed at high concentrations in solutions of very flexible polymers.[54] The origin of these modes is not yet known, although several explanations have been proposed.[54-56]

The most likely explanation of the observed trends of most of the data involves the onset of rotational translational coupling at higher concentrations. The coupling arises because the translational diffusion coefficient perpendicular to the molecular axis ($D_\perp$) becomes much smaller than that parallel to the axis ($D_\parallel$) because of the hindering of the perpendicular motion due to molecular caging. This is basically the mechanism of the original Doi-Edwards theory.[1-3] The magnitude of the translational rotational coupling depends on a parameter

$$\gamma = q^2(D_\parallel - D_\perp)/\theta$$

where θ is the rotational diffusion coefficient. Doi and Edwards[4] computed the polarized correlation function in the limit of γ equal infinity. Since the amount of slowing down of the rotational diffusion coefficient was generally found to be less than that predicted by Doi-Edwards, the value of γ in most cases of interest is relatively small. Zero and Pecora[46] modified the theory to show how rotational translational coupling could give rise to multiple relaxation modes in the polarized DLS time correlation function even for relatively small values of γ. Zero and Pecora[46] showed that the first mode in the polarized spectrum has a re-

laxation time approximately at q^2D, a second mode at $q^2D + 6\theta$ and other weaker faster modes that become more important as γ becomes larger. Aragon and Pecora[57] solved the general case of arbitrary γ including the effects of molecular form factors and found results which in the limits of small and large γ agree with those previously found. As γ increases, the modes present can slow down greatly but all modes should be faster than the slowest mode that, in the absence of thermodynamic nonideality effects, slows continuously with increasing γ from the value of q^2D at $\gamma = 0$. This qualitatively describes the trends in our DLS data.

Precise evaluation of the rotational–translational coupling parameter γ is difficult since it depends on the ratio of two unknowns. Estimates of these unknowns are complicated by questions of flexibility, solution thermodynamic nonideality effects, and possible alternative cage dissipation mechanisms. However, rough estimates of γ may be made to show that it may be sufficiently large so that it could give rise to the complex multiple mode structure as observed in our data.

Zero and Pecora[46] calculated the DLS time correlation functions to second order in γ and estimated that their approximations are valid up to about $\gamma = 10$. At higher values of γ higher order terms start to become significant. We cannot measure $\Delta D \equiv D_\parallel - D_\perp$ directly so that some simplifying assumptions must be made. If it is assumed as in the original Doi–Edwards theory that motion perpendicular to the rod axis is completely prevented while motion parallel to it is unaffected, then $\Delta D \approx {}^2/_3 D$. Furthermore, if the Broersma relation is used to calculate the rotational diffusion coefficient in dilute solution, then $q^2D \sim 6\theta_0$ and $\gamma \sim 4$. The rotational diffusion coefficient in the semidilute region should, however, be less than the dilute solution value, so it is expected that γ will be even larger than the 4. If it is assumed that the difference in time scales for the first two modes in the polarized DLS correlation function is 6θ, as it is for small γ,[46] then θ falls by a factor of 2–20 (depending on the sample and concentration) in which case γ is in the range of 8 to 80.

An alternative estimate of γ may also be made. Ignoring thermodynamic nonideality effects, the primary mode should have a decay constant $\Gamma = q^2D - (2/135)\theta\gamma^2 + \ldots$. The data indicate that the primary mode becomes slower by a factor of 1.5–2.5 as the concentration increases (except for the enigmatic case of the small PHIC with its very slow mode). If one assumes that $q^2D \sim 6\theta_0$, then we have $\gamma \sim$ 12–16. If it is assumed that D does not change and that θ changes by the factor of 2–20 found from the mode spacing, then γ goes up by a factor of the square root of 2–20 to give a final estimate in the range between 17 and 72.

In any event these rough estimates place γ in the range of 10–100 for the various high C solutions so that translational rotational coupling can give at least a consistent explanation for the appearance of the multiple fast modes in the DLS time correlation functions except for the small PHIC, which as we noted in section IV could have ordered aggregates present that indicate that this sample is near the composition for a transition to a liquid crystalline phase. If this is the case, it might be expected that the POIC sample which has a similar length and a larger diameter should display similar behavior. Indirect evidence, however, based on the flow behavior (Tables I and IV) indicates that the POIC may be more flexible than the small PHIC.

Assuming that rotational–translational coupling is the origin of the primary and secondary modes, the concentration dependence of θ may be deduced from the concentration dependence of the difference of the reciprocal decay times of the secondary and primary modes. The results are presented in Table VII. Rotational diffusion coefficients obtained in this manner are, of course, not very precise, but they give better estimates than those obtained from the more noisy depolarized data (which are not presented here in detail).[28] In Table VII, the rotational diffusion coefficients are presented relative to values calculated from the Broersma equation for rigid rods using the parameters given earlier. The ratio of the Broersma value to the measured value is given since it represents the factor by which the rotation is slowed by interactions assuming the theoretical dilute solution value. Although there is much scatter in these necessarily rough estimates, they vary in a suggestive way. The big PHIC (which is the most flexible because of its greater length) yields ratios in the 1–3 range indicating a small deviation from the expected dilute solution behavior. The small PHIC at the lower concentrations studied shows similar results before the appearance of the slow mode. The other samples show ratios of the order of 10–20 (with very little concentration dependence).

Any concentration dependence that might be present is lost in the scatter of the data except for the fact that the very lowest concentrations exhibiting two modes of each series show a lesser degree of slowing, of a factor of

Table VII
Ratio of θ Calculated for Rod in Dilute Solution to θ Measured Assuming the First Two Polarized Modes Correspond to q^2D and $q^2D + 6\theta$[a]

concn			θ(calcd)/θ(measd)	
(mg/mL)	CL^3	CL^2d	T = 20 °C	T = 40 °C
		POIC		
19.4	91	2.11	13	
7.5	35	0.81	14	
4.5	21	0.49	18	
2.8	13	0.30	11	
1.8	8.4	0.20	8	
		Big PHIC (Dry)		
3.4	83	0.72	2.3	1.4
1.9	47	0.40	1.6	2.1
1.1	27	0.23	0.60	2.4
0.54	13	0.12	0.92	0.94
0.30	7.4	0.064	0.87	0.63
0.13	3.2	0.028	1.3	
		Big PHIC (Wet)		
11	270	2.34	2.6	
10	245	2.13	1.9	
2.65	65	0.56	2.1	
2.17	53	0.46	2.1	
1.5	37	0.32	1.6	
0.66	16	0.14	1.8	
		PBIC (Chloroform)		
11	75	1.00	11	
9.6	65	0.87	14	
5.9	40	0.54	12	
5.2	35	0.47	14	
2.8	19	0.25	14	
1.36	9.3	0.12	3.9	
		Small PHIC		
34	22	0.37	2.8	
2.8	18	0.31	2.0	
		PBIC (Cyclohexane)		
0.6	4.1	0.054	17	
0.375	2.6	0.034	20	
0.085	0.58	0.0077	5	

[a] Numbers greater than one indicate a slowing of rotational motion as compared to the theoretical dilute solution values.

only 4–8. This is strongly indicative of a rapid decrease in θ as rotational–translational coupling sets is followed by a large concentration region in which θ is constant.

It might be suggested that the absolute values of these ratios for the slowing down of the rotational motion are due to errors in the estimates of the rod lengths used to calculate the dilute solution values. Since the dilute solution diffusion coefficient scales as the third power of L, an error of a factor of 2.5 would suffice to say that there is no slowing down of the rotation and that the θ measured is approximately the same as for the dilute solution. The rather low value of θ for the big PHIC might then be ascribed to its high flexibility. Such an interpretation is, however, not consistent with the lower concentration data. In any case the conclusion remains that in most of the region studied no concentration dependence of θ was observed.

The simplest interpretation of these observations is that there is a transition in the value of θ that corresponds to the onset of caging. This caging is manifested in the polarized time correlation function through translational–rotational coupling. The apparent lack of a concentration dependence of θ in this higher concentration region is in qualitative agreement with the theories of Odijk[6] and Doi[8] for the reptational motion of entangled wormlike coils, providing that a liquid crystal or microgel does not result at high concentrations. In these concentration regimes, the rotational motion is not limited by cage size but by the ability of the molecule to bend to a new cage as it translates along its length—more of a reptational motion than the usual picture of rodlike motion. As can be seen from the theoretical analysis in section II, such a concentration regime is difficult to avoid and we believe that this is what we are seeing in these solutions at the higher concentrations.

VI. Summary

A concise summary of the rather complex behavior suggested by these experiments follows.

At low concentrations, the translational and rotational diffusion of these molecules is much as predicted by the dilute solution theories. When a certain critical concentration range is reached, two related effects occur due to caging: (1) translational diffusion becomes more anisotropic and (2) rotational diffusion is slowed. These effects are indicated by a splitting of the modes from a single exponential to a series of modes extending to fast times, with the intensity transferring from the original slowest mode to the faster modes with increased concentration. The modes slow down in concert, but the intensity-weighted average of these modes remains at a constant position or shifts in either direction to reflect whatever thermodynamic nonideality effects may be present. The spacing of the modes narrows to reflect the slowing down of the rotational diffusion.

This narrow concentration regime crosses into a regime in which the rotational diffusion coefficient is relatively independent of concentration. This occurs when the flexing motion of a macromolecular chain becomes larger than the cage size (see section II). The actual amount of rotational slowing in this regime depends on the rigidity of the rods.

The next manifestation is a falling of the polarized scattering intensity per molecule, indicative of significant thermodynamic nonideality effects. This is followed at higher concentrations by increased depolarized scattering, indicating some orientational ordering. These occur because the rods do not fit in the confines of their cages (again see the theory in section II).

The ultimate behavior of the system at the very highest concentrations depends upon the particular polymer studied. If the rods are sufficiently rigid or insoluble, a liquid crystal or gel will form. If the rods are sufficiently flexible, solutions of very high concentrations can be prepared. The small PHIC and PBIC are examples of the former and the POIC and wet big PHIC are examples of the latter.

It is clear that much more experimental and theoretical work must be done on these systems to make this qualitative picture more precise. In particular, the various mechanisms for translational and rotational motion in entangled semiflexible rodlike systems should be a focus for future work. The interplay of reptation and cage dissipation must be better understood as well as any effects that cage formation might have on the internal dynamics and conformations of wormlike coils.

Acknowledgment. This work was supported by the NSF MRL Program through the Center for Materials Research at Stanford University and by NSF Grant CHE85-11178. We are grateful to Dr. S. M. Aharoni of Allied Corp. for kindly providing the poly(n-alkyl isocyanate) samples used in this work. They are also grateful to Professor S. R. Aragon of San Francisco State University for suggesting that we study these systems and for help in the initial stages of this work.

Registry No. PBIC, 25067-04-3; PHIC, 26746-07-6; POIC, 32646-75-6.

References and Notes

(1) Doi, M. *J. Phys. (Les Ulis, Fr.)* **1975**, *36*, 607; *J. Polym. Sci., Polym. Phys. Ed.* **1981**, *19*, 229; *J. Chem. Soc., Faraday Symp.* **1983**, *18*, 49.
(2) Doi, M.; Edwards, S. F. *J. Chem. Soc., Faraday Trans. 2* **1978**, *74*, 560, 918.
(3) Edwards, S. F. *J. Chem. Soc., Faraday Symp.* **1983**, *18*, 145.
(4) Flamberg, A.; Pecora, R. *J. Phys. Chem.* **1984**, *88*, 3026.
(5) Teraoka, I.; Ookubo, N.; Hayakawa, R. *Phys. Rev. Lett.* **1985**, *55*, 2712.
(6) Odijk, T. *Macromolecules* **1983**, *16*, 1340; **1984**, *17*, 502.
(7) Odell, J. A.; Atkins, E. D. T.; Keller, A. *J. Polym. Sci., Polym. Lett. Ed.* **1983**, *21*, 289; *Macromolecules* **1984**, *18*, 1443.
(8) Doi, M. *J. Polym. Sci., Polym. Symp.* **1985**, *73*, 93.
(9) Keep, G. T.; Pecora, R. *Macromolecules* **1984**, *18*, 1167.
(10) Edwards, S. F.; Evans, K. E. *J. Chem. Soc., Faraday Trans. 2* **1982**, *78*, 113.
(11) Onsager, L. *Ann. N.Y. Acad. Sci.* **1949**, *51*, 627.
(12) Flory, P. J. *Proc. R. Soc. London, Ser. A* **1956**, *234*, 73.
(13) Pecora, R. *J. Polym. Sci., Polym. Symp.* **1985**, *73*, 83.
(14) Kratky, O.; Porod, G. *Recl. Trav. Chem. Pays-Bas* **1948**, *68*, 1106.
(15) Yamakawa, H.; Fujii, M. *Macromolecules* **1973**, *6*, 407; Fujii, M.; Nagasaka, K.; Shimada, J.; Yamakawa, H. *Macromolecules* **1983**, *16*, 1613.
(16) Dung, M. H.; Ladanyi, B. M. *Macromolecules* **1984**, *17*, 1238.
(17) Fujime, S.; Maeda, T. *Macromolecules* **1985**, *18*, 191.
(18) Aragon, S. R.; Pecora, R. *Macromolecules* **1985**, *18*, 1868. Aragon, S. R. *Macromolecules* **1987**, *20*, 370.
(19) Fixman, M. *Phys. Rev. Lett.* **1985**, *54*, 337; **1985**, *55*, 2429.
(20) Frenkel, D.; Maguire, J. F. *Phys. Rev. Lett.* **1981**, *47*, 1025; *Mol. Phys.* **1983**, *49*, 503.
(21) Magda, J. J.; Davis, H. T.; Tirrell, M. *J. Chem. Phys.* **1986**, *85*, 6686.
(22) Mori, Y.; Ookubo, N.; Hayakawa, R.; Wada, Y. *J. Polym. Sci., Polym. Phys. Ed.* **1982**, *20*, 2111.
(23) Bur, A. J.; Fetters, L. J. *Chem. Rev.* **1976**, *76*, 727.
(24) Bur, A. J.; Roberts, D. E. *J. Chem. Phys.* **1969**, *51*, 406. Bur, A. J. *J. Chem. Phys.* **1970**, *52*, 3813.
(25) Schneider, N.; Furusaki, S.; Lenz, R. *J. Polym. Sci., Part A* **1965**, *3*, 933.
(26) Tonelli, A. *Macromolecules* **1974**, *7*, 628.
(27) Aharoni, S. M. *Macromolecules* **1979**, *12*, 94.
(28) Keep, G. T. Ph.D. Thesis, Stanford University, 1986.
(29) Cantow, M. J. R., Ed. *Polymer Fractionation*; Academic: New York, 1967.
(30) Rubingh, D.; Yu, H. *Macromolecules* **1976**, *9*, 681.

(31) Statman, D.; Chu, B. *Macromolecules* **1984**, *17*, 1537.
(32) Riseman, J.; Kirkwood, J. G. *J. Chem. Phys.* **1950**, *18*, 512. Kirkwood, J. G.; Auer, P. L. *Ibid* **1951**, *19*, 281.
(33) Ambler, M.; McIntyre, D.; Fetters, L. J. *Macromolecules* **1978**, *11*, 300.
(34) Berger, M.; Tidswell, B. M. *J. Polym. Sci., Polym. Symp.* **1973**, *42*, 1063.
(35) Broersma, S. *J. Chem. Phys.* **1960**, *32*, 1626, 1632; **1981**, *74*, 6989.
(36) Lewis, R. J. Ph.D. Thesis, Stanford University, 1985.
(37) Russo, P. S.; Miller, W. G. *Macromolecules* **1984**, *17*, 1324.
(38) Bersted, B. *J. Appl. Polym. Sci.* **1973**, *17*, 1415.
(39) Marrucci, G.; Grizzuti, N. *J. Polym. Sci., Polym. Lett. Ed.* **1983**, *21*, 83.
(40) Maier, K. R. Ph.D. Thesis, Stanford University, 1986.
(41) Provencher, S.; Hendrix, J.; DeMayer, L. *J. Chem. Phys.* **1978**, *69*, 4273. Provencher, S. *Makromol. Chem.* **1979**, *180*, 201; *Comput. Phys. Commun.* **1982**, *27*, 213, 229.
(42) Bott, S. E. In *Measurement of Suspended Particles by Quasi-Elastic Light Scattering*; Dahneke, B., Ed.; Wiley: New York, 1983; Ph.D. Thesis, Stanford University, 1984.
(43) Malmberg, M. S.; Lippincott, E. R. *J. Colloid Interface Sci.* **1968**, *27*, 591. Huglin, M. B., Ed. *Light Scattering from Polymer Solutions*; Academic: London, England, 1972.
(44) Russo, P. S.; Langley, K.; Karasz, F. E. *J. Chem. Phys.* **1984**, *80*, 5312.
(45) Jamieson, A.; Southwick, J.; Blackwell, J. *J. Polym. Sci., Polym. Phys. Ed.* **1982**, *20*, 1513.
(46) Zero, K. M.; Pecora, R. *Macromolecules* **1982**, *15*, 87.
(47) Aharoni, S. M.; Walsh, E. K. *Macromolecules* **1979**, *12*, 271. Aharoni, S. M. *J. Polym. Sci., Polym. Phys. Ed.* **1980**, *18*, 1303, 1439.
(48) Kubota, K.; Chu, B. *Biopolymers* **1983**, *22*, 1461.
(49) Kubota, K.; Chu, B. *Macromolecules* **1983**, *16*, 105.
(50) Pecora, R. *J. Chem. Phys.* **1968**, *48*, 4126; **1968**, *49*, 1032.
(51) Pusey, P. N.; Fijnaut, H. M.; Vrij, A. *J. Chem. Phys.* **1982**, *77*, 4270.
(52) Lee, W. I.; Schmitz, K. S.; Lin, S.-C.; Schurr, J. M. *Biopolymers* **1977**, *16*, 583.
(53) Hartl, W.; Versmold, H. *J. Chem. Phys.* **1984**, *80*, 1387.
(54) Han, C. C.; Schaefer, D. W. In *Dynamic Light Scattering: Applications of Photon Correlation Spectroscopy*; Pecora, R., Ed.; Plenum: New York, 1985.
(55) Brown, W. *Macromolecules* **1984**, *17*, 66.
(56) Balloge, S.; Tirrell, M. *Macromolecules* **1985**, *18*, 817.
(57) Aragon, S. R.; Pecora, R. *J. Chem. Phys.* **1985**, *82*, 5346.

Phase Separation in Ternary Systems Solvent–Polymer 1–Polymer 2. 3. Homogeneous Double Critical Points

K. Šolc* and Y. C. Yang

Michigan Molecular Institute, Midland, Michigan 48640. *Received June 2, 1987*

ABSTRACT: A number of quantitative relations have been developed for homogeneous double critical points (HODCP's) in Flory–Huggins ternary systems solvent–polymer 1–polymer 2 with interactions characterized by polymer–polymer parameter g_x and solvent–polymer parameters g_1 and g_2. Their location in the composition diagram is restricted to three linear segments, and they can exist only for combinations of g_x and Δg ($\Delta g \equiv g_2 - g_1$) limited to double-sector areas of the $g_x,\Delta g$ plane. The lower sectors contain exclusively *elliptic* HODCP's marking disappearance of closed-loop binodals, while the upper sectors are divided between *hyperbolic* (marking confluence of two binodal regions) and *unstable elliptic* types. Sector vertices represent unique systems where the effect of unequal chain lengths is just balanced by interactions to produce a constant critical temperature, independent of composition. Conditions for multiple occurrence of HODCP's and relations for orientation of spinodals at HODCP's are derived. Special attention is paid to systems located on hyperbolic boundaries between elliptic and hyperbolic regions where HODCP's overlap with heterogeneous double critical points. A criterion is also given for improving the solvent power in terms of interaction parameter perturbations.

1. Introduction

Homogeneous double critical points (HODCP's) in ternary systems mark conspicuous changes in the pattern of isothermal spinodals and binodals. In one instance (which might be called *elliptic*) it is the disappearance from the phase diagram of loop-shaped binodals that defines closed, usually two-phase regions (sequence T_3, T_2, T_1, T_0 in Figure 1); in the other case (*hyperbolic*), two regular growing two-phase regions coalesce into a single two-phase region without a critical point (sequence T_2, T_1, T_0, T_{-1} in Figure 2). In both instances two real single critical points of the same kind approach each other with changing temperature, merge into a HODCP at T_0, and become complex (i.e., disappear from the real space).[1,2]

So far the occurrence of HODCP's has been studied only for two simple extreme cases: (i) they were detected in regular ternary solutions whose components differ in interactions but not in molecular volumes;[3] (ii) it has also been shown that they *cannot* exist in quasi-binary solutions whose polymeric components differ but by their chain lengths.[4] Thus some degree of disparity in interactions between the three components seems necessary for their appearance. On the other hand, the chain-length effect, although by itself incapable of producing the HODCP's, will certainly modify their location in the space of variables if combined with the difference in interactions. In order to gain quantitative knowledge about the interplay of these two factors, the conditions are here examined for the existence of HODCP's in general Flory–Huggins ternary systems solvent (0)–polymer (1)–polymer (2). A preliminary report on this subject was given in ref 5.

2. Critical State Conditions

The critical state in the examined system is defined by the following three functions:[2,6]

$$F_c \equiv \Phi^2\langle r\xi\rangle^3 - \langle r^2\xi^3\rangle = 0 \tag{1}$$

$$G_c \equiv \xi^2(1 - \varphi_2 r_2 P) - (1 - \varphi_1 r_1 M) = 0 \tag{2}$$

$$H_c \equiv \xi^2 + 1 + \varphi\{\xi\langle r\xi\rangle[(2/\varphi_0) - 4\bar{g}] + w_1 r_1 P + \xi^2 w_2 r_2 M\} = 0 \tag{3}$$

where φ_i is the volume fraction of the component i, with φ being the total volume fraction of the polymeric solute, $\varphi = \varphi_1 + \varphi_2$; Φ stands for the ratio $\Phi = \varphi/\varphi_0$; the construct $\langle\ \rangle$ denotes the moment

$$\langle r^i\xi^j\rangle = w_1 r_1{}^i\xi^{-j} + w_2 r_2{}^i\xi^j$$

where $w_m = \varphi_m/\varphi$, $m = 1, 2$, are the volume fractions of

0024-9297/88/2221-0829$01.50/0